# SOME IMPORTANT ISSUES OF MIL AND LFD ANISOTROPY MEASURES THAT USERS ARE USUALLY NOT CONSCIOUS

**Krzysztof Janc***, **Jacek Tarasiuk***, **Pawel Lipinski†**, **Anne-Sophie Bonnet†**, **Sebastian Wronski***

*AGH University of Science and Technology, Faculty of Physics and Applied Computer Science
al. Mickiewicza 30, 30-059 Kraków, Poland
tarasiuk@agh.edu.pl, wronski.sebastian@gmail.com

† Université de Lorraine, Ecole Nationale d'Ingénieurs de Metz, Département de Mécanique,
Physique et Mathématiques
1 route d'ARS LAQUENEXY, BP 65820, 57 078 METZ CEDEX 03
pawel.lipinski@univ-lorraine.fr, anne-sophie.bonnet@univ-lorraine.fr

**Keywords:** Anisotropy Measures, Line Fraction Deviation, Mean Intercept Length.

**Abstract:** *Trabecular bone tissue, vascular system, alveoli, polymer scaffolds, metallic foams absorbing impact energy, some minerals and rocks are examples of porous objects with pronounced micro-architectures. Last years, thanks to sudden development of X-ray tomography and micro-tomography, methods to quantify its anisotropy are frequently applied. Classical 2D methods are also expanded to 3D situations. Two very widely used methods, namely Mean Intercept Length and Line Fraction Deviation, have some drawbacks that users are usually not conscious. The source of the problem lies in the discrete (rasterized or pixelized) nature of computer images. This work is dedicated to improvement of both methods and overcome their limitations.*

## 1  INTRODUCTION

The microstructure of composite and porous materials has a large influence on their global mechanical properties [1]. Adding reinforcements to the polymer matrix, such as for instance randomly distributed fly ash, can substantially change its effective mechanical behavior. In such a case, isotropic properties are usually obtained, that means values of mechanical properties are independent from the direction of mechanical testing. The situation becomes completely different when elongated reinforcements, such as fibers, are mainly oriented in the same direction. Consequently, the resulting mechanical properties of the material have a more complex anisotropy. In the case of porous materials, the situation is similar. Pores can be represented more or less accurately by ellipsoids. If the pores shapes are close to spheres and they are randomly distributed, then porous materials exhibit isotropic properties. On the other hand, if the pores are close to an ellipsoidal shape with a high ratio of their semi-axes arranged along specific directions, then the material becomes anisotropic.

Porous materials with anisotropic properties are frequently encountered in biomechanics. This concerns mechanical properties of bones as well as diffusion properties of soft tissues [2,3]. As first explained by Meyer [4] and Wolff [5] in the second half of the 19th century, it

is because the inner structure of the bone tissue adapts to the local distribution of stresses and strains. Bone tissue has the ability to rebuild its microstructure to provide the most effective properties with the minimum weight. To predict the global behavior of such tissues, their micro-architecture must be studied. Knowledge of these properties has a major socioeconomic importance, because it enables the determination of bone quality and fracture risk in bone diseases and implant solutions [6]. The pioneering works on the evaluation of anisotropic microstructures already appeared before 1940. These methods were developed to measure and describe the internal structure of granular and porous materials. In polished cross-sections of such materials, the interface surface between the constituents becomes clearly visible. Samples of the material are studied with a microscope equipped with measuring grids consisting on parallel lines. By counting how many times, for a given direction of grid lines, the sampling lines intersect with the interfaces, the material anisotropy can be quantified.

In the last years, development of micro-computed tomography (μ-CT) gave a huge opportunity to study three-dimensional microstructures. Based on a series of 2D scans made at different angles and using computer algorithms, a complete reconstruction of the internal structure of the material can be done. There exist several methods enabling the description of material anisotropy from μ-CT data. The Mean Intercept Length (MIL) [7], Line Fraction Deviation (LFD) [8], Volume Orientation (VO) [9], Star Volume Distribution (SVD) [10] or Star Length Distribution (SLD) [11] belong to the most popular approaches.

All these methods are very commonly used both in research and medical applications. For example, the quantification of trabecular bone tissue anisotropy is usually based on such approaches. The issues that concern these approaches will become more and more important with increasing resolution of the medical imaging systems. Another large field of use of the methods is to develop a relationship between morphology and mechanical properties of trabecular bone. For instance, Zysset [12] developed a tactic based on the MIL method. His methodology is still widely used. Also, the very popular free software ImageJ, with the BoneJ plugin for bone analysis, utilizes MIL method for anisotropy description. Usually, the imperfections found in the MIL or LFD methods only have a small influence on the final results. But in some special circumstances, they may lead to significant distortions of the anisotropy characterization. A large part of the authors using these methods is not aware of their glitches resulting from the numerical interpretation of the images on a computer.

In this paper first, the bases of MIL and LFD methods are presented followed by the identification of their respective defaults related to the image pixelization. Next is devoted to the description of the improvements of these methods, which enable overcoming the identified problems

## 2 ANISOTHROPY MEASURES

### 2.1 Mean Intercept Length (MIL)

One of the most popular methods for determining the structural anisotropy of the material is the Mean Intercept Length method. Whitehouse [7] introduced first this method to quantify the anisotropy of materials consisting of two phases. To determine the value of MIL for a given image, one has to use a grid consisting of a series of parallel sampling lines covering the tested image (see Fig.1). Then for each line, the number of intercepts is calculated, namely the occurrences where the phase changes. As specified by the following formula, the measure of MIL, for a given angle ϕ, is the ratio of the whole length L of all the sampling lines divided by the entire number of phase change counts I(ϕ) of a given orientation:

$$MIL(\phi) = \frac{L}{I(\phi)} \qquad (1)$$

Usually, the MIL($\phi$) values are calculated for line angles rotated every each 5° in the range: 0≤$\phi$≤180°. To obtain the full information on anisotropy, for 180°<$\phi$≤360° the relation: MIL($\phi$)=MIL($\phi$-180°) is used.
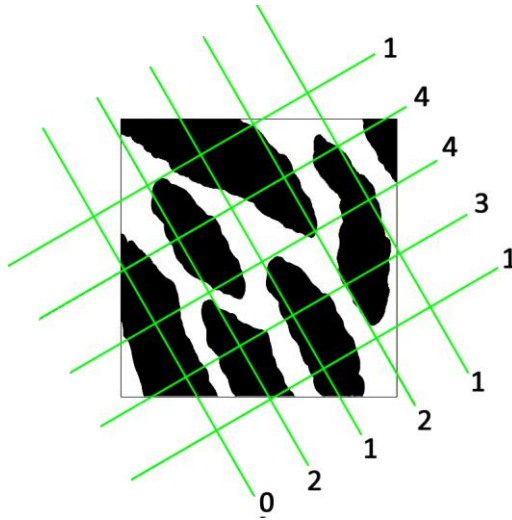


Figure 1: The idea of the anisotropy measurement with the MIL method. Two different positions of grid lines are presented. The numbers at the ends of sampling lines indicate the number of phase changes for each line (only changes from white to black phase are counted).

Usually, the anisotropy of analyzed images is plotted on a polar chart. In this paper, the obtained anisotropy measures are normalized in the way that the maximum anisotropy value is equal to one and corresponds to the radius of the chart. The obtained graphs are next enveloped by an ellipsis. Obviously, isotropic structures are represented as circles on such plots. A strong anisotropy is depicted by narrow ellipses. The orientation of the long axis of the ellipsis a indicates the main direction of anisotropy. The degree of anisotropy DA is defined by the relation:

$$DA = 1 - \frac{b}{a} \qquad (2)$$

where *b* is the second (small) semi axis of the ellipsis.

An example of anisotropy evaluation by the MIL method is presented in Fig. 2., where the radius of the plot is normalized by the maximal value of MIL. The qualitative interpretation of the results obtained by the MIL method is quite simple: the more flattened the ellipse on the plot, the stronger anisotropy on the image analyzed and the bigger the value of DA. As mentioned above, the main direction of anisotropy (stacking structures along one direction) is equivalent to the direction of the long semi-axis of the ellipsis.

## 2.2 Line Fraction Deviation (LFD)

The Line Fraction Deviation (LFD) method was developed at the Department of Dental Radiology of ACTA, to measure the orientation on radiographic trabecular patterns. It was tested on archives of radiographs already existing at the department; the results were published by Geraets [13] and Korstjens [14]. Similarly, to the MIL method, in the LFD approach, a grid is applied. The difference is that, in the case of LFD method, the phase fraction is calculated for every line independently. The fraction should be understood as the ratio of the length of the image tested phase lying along the grid line, to the entire length of this line. After determining the phase fraction for all parallel grid lines at a given direction, a standard deviation of the fraction is calculated for each direction. This value of standard deviation defines the LFD value

calculated for each orientation angle $\Phi$ of parallel lines. Analogously as in the MIL method, one can represent the results in the form of a polar diagram (Fig. 3).
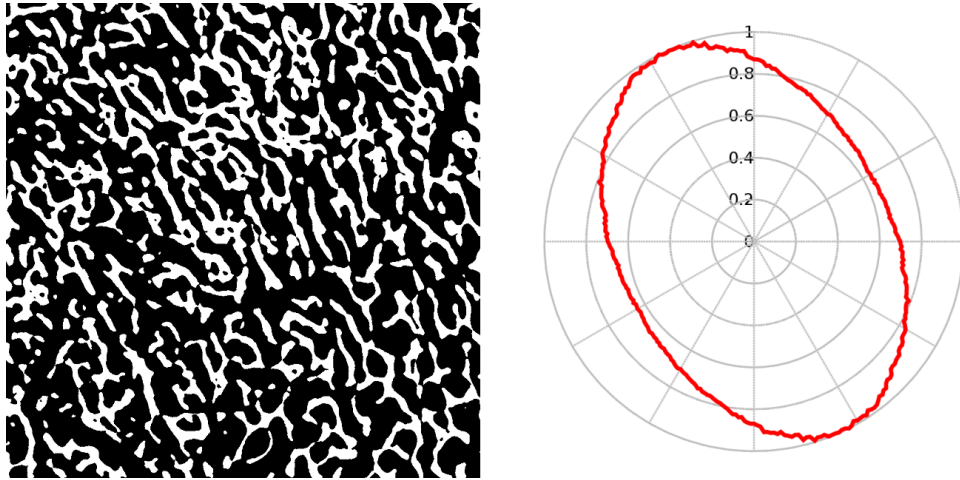


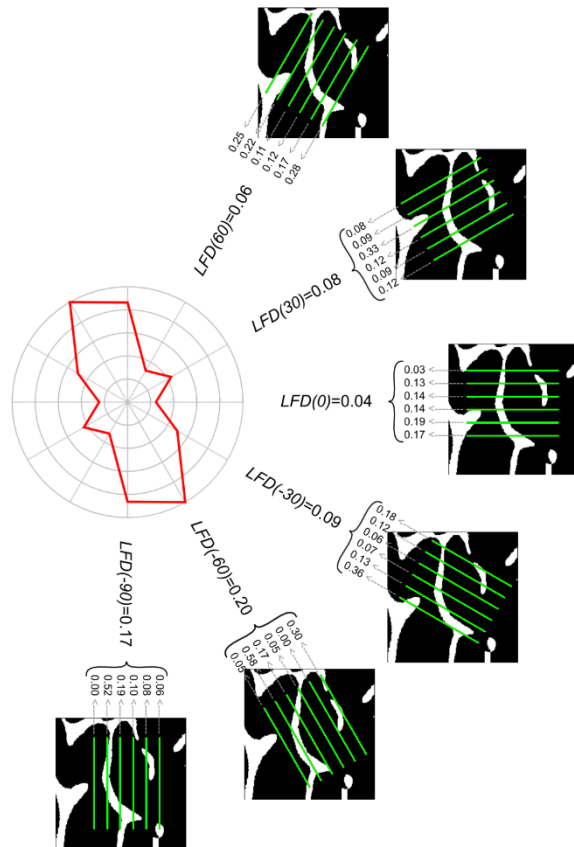Figure 2: MIL value as a function of the angle φ for a typical cancellous bone image.



Figure 3: The idea of the LFD method. Several grids of sampling lines at various angles are presented. For each orientation, standard deviation of phase fraction for all lines is calculated.

However, the charts obtained by these two methods can be significantly different. Figure 4 shows a comparison of both methods in the case of specially prepared testing images constituted of white ellipses and black background.
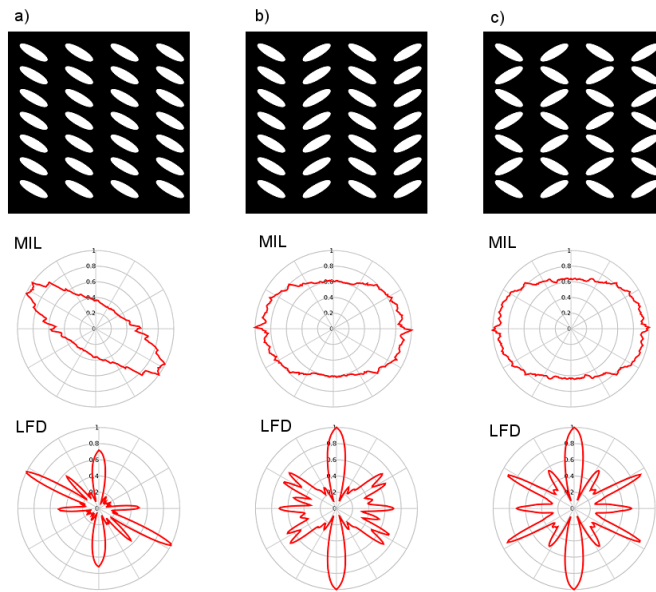
Figure 4: Comparison of anisotropy quantification by MIL and LFD methods for testing images. In the top row, the testing images are presented. In the middle and bottom rows are drawn the resulting MIL and LFD charts, respectively.

It can be seen that MIL method only recognizes global anisotropy. For test image (a), both methods give similar results concerning the main direction of anisotropy but LFD detects also a vertical anisotropy that corresponds to the organization of white ellipses in columns. Test images (b) and (c) characterized by MIL are almost identical and predict a relatively low anisotropy. LFD method differentiates the main and secondary anisotropy directions. The main directions of anisotropy (LFD=1) are due to the global organization of ellipses. The secondary ones correspond to the local orientations and shapes of ellipses. Both methods are frequently used in spite of their specific drawbacks.

## 3 PROBLEMS AND ISSUES

### 3.1 Discretization problem in MIL method

The main problem with the MIL method consists in its high sensitivity to the roughness of the boundary (interface line) between two phases. If a very rough boundary between phases lies along the grid line, it can cause a significant increase in the global number of phase changes, which is not always connected to real anisotropy (see Fig. 5).
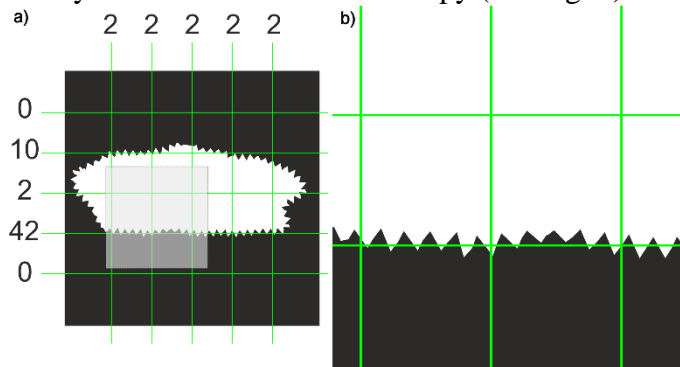


Figure 5: a) Rough object with sampling lines. The numbers on the ends of the lines indicate counts of the phase changes. b) Zoom on the rough boundary at the interface.

5

The problem is especially pronounced in the computer digital representation of the image where pixelization (or rasterization) leads to a rough boundary even if the real boundary is smooth. The roughness of the phase interfaces and sampling lines depends on the orientations of the object according to the image raster (Fig.6).

The following color convention is adopted in this paper; the pixels constituting the scanning lines are marked in red if they are in the white phase and in blue if they are located in the black phase on the black and white prints, red will appear as dark gray and blue as light gray.
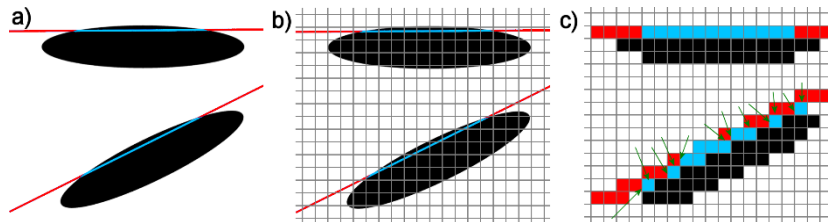


Figure 6: a) Example of ideal ellipses in two different orientations with smooth edges and smooth sampling lines. b) Raster applied to the ideal image. c) Zoom of rasterized ideal image. The ellipses are in black. Pixels of sampling line lying outside the ellipses are painted red and pixels inside ellipses are in blue (dark grey and light grey respectively on B&W prints). For the top ellipsis, the MIL algorithm counts only two intercept points, whereas for the inclined one 12 intercept points) were found.

Let's consider an ideal elliptical shape as one object embedded in a black background (see Fig. 7a and 7b). The two black and white images of this figure were prepared with the ellipsis oriented horizontally and counter-clockwise rotated 45° about its center. The dimensions of the images are 250 x 250 pixels. The anisotropy chart calculated by the conventional MIL method gives two different plots (Fig. 7c). As expected, the second one is rotated 45° to the first one but the shapes of the two plots are significantly different. This is a straight example of the rasterization effect on the number of intercepts counts.
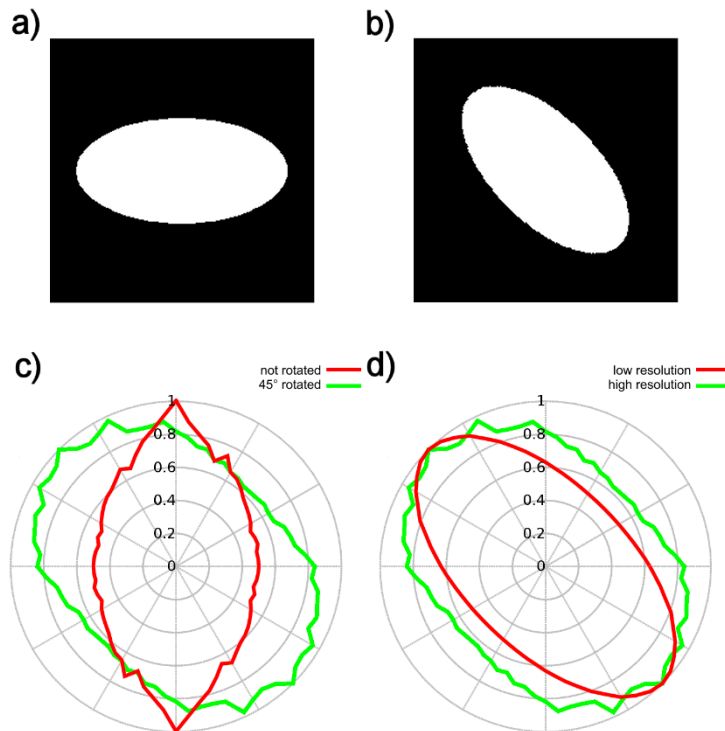


Figure 7: Two phases images with a) vertical and b) 45°-rotated ellipsis. c) Anisotropy MIL plots for vertical

and rotated ellipses. d) Anisotropy MIL plots of rotated ellipsis for low and high resolution images.

Also, the resolution of the images influences the results. In the next example, the rotated ellipsis image of Fig 7b was prepared in the high resolution of 2500 x 2500 pixels. The comparison of the plots for low and high-resolution images is shown in Fig. 7d. Higher resolution weakens the effect of rasterization, what is a common situation in raster graphics images.

Another problem, which occurs in the MIL method, is the fact that the phase boundary may be straight and parallel to the lines of the grid. The results obtained strongly depend on the location of the sampling lines. The numerical, discreet representation of the image leads to the situation that two parallel or nearly parallel lines can cross each other periodically (Fig. 8). The value of the intervals, in which the straight lines cross, depends on the angle. For the angles being multiples of 45˚, this effect never occurs. For other slopes, the importance of the effect depends on the angle and the structure tested. Consequently, the MIL values have tendency to be diminished for all directions except of 45˚ and its multiples.
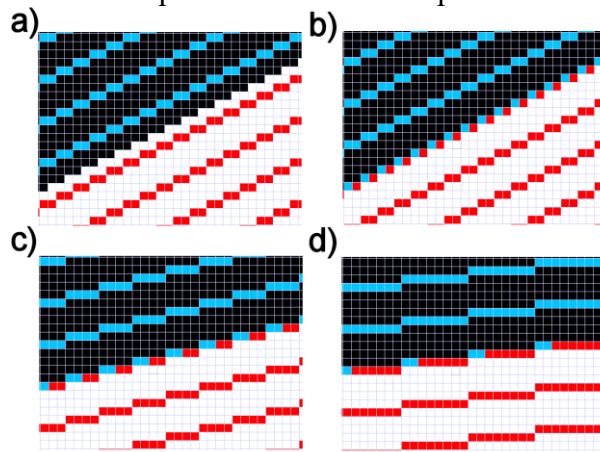


Figure 8: The picture represents the simple linear border between two phases depending on the selection of the measurement grid. a) the best situation: border and sampling lines are parallel and 45° oriented b-d) an effect of the error caused by numerical representation of the straight line in the image depending on the orientation of the boundary.

In MIL, only the changes between two phases are counted. In practice, any points with two neighboring pixels having different colors are treated as an interface between phases. The adverse location of pixelized line and pixelized phase boundary may lead to improper phase intersect counts. The described faults of the MIL method usually don't change the main directions of anisotropy but may have a strong influence on the shape of the anisotropy plot. Unconsciousness of the problem may be especially risky if comparing various images with different raster orientations or resolutions.

## 3.2 Limitations of LFD method

In LFD method, the analyzed area is always smaller than the images. Typical practice is to create square shaped regions filled with parallel sampling lines to provide that the grid is always entirely inside the image, independently of its orientation.

This procedure causes that the tested area for a given angle is limited only to the square inside the circle whose diameter is equal to the edge of the image (Fig. 9). The regions on the image outside the circle are never analyzed and have no incidence on the anisotropy chart.
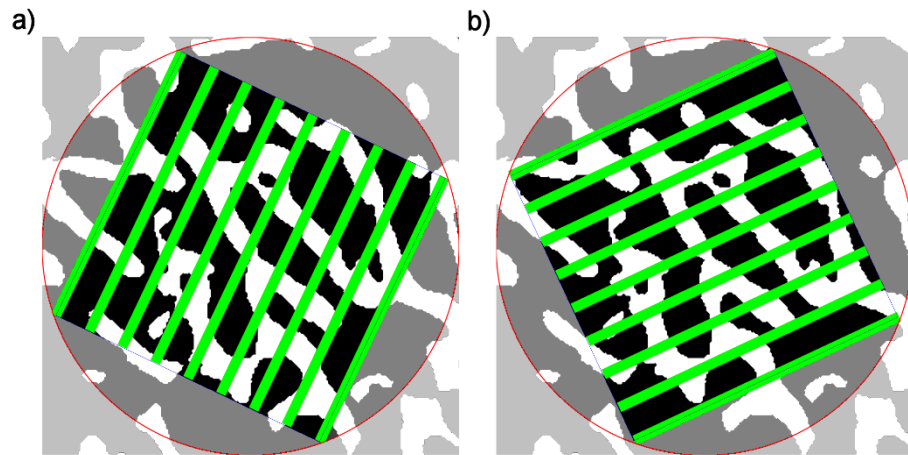
Figure 9: Appearance of the test grid used in the LFD method for two selected angles. The corners in light grey are never analysed by the method. The parts in dark grey are analysed only partially depending on grid orientation.

Moreover, depending on the grid orientation, various parts of the image come into the analyzed square. It means that the results may be not consistent because the LFD computations for various angles take into account different regions. In consequence, the rotation of the structure may lead to different anisotropy charts. To verify this assertion, a numerical experiment has been done. The LFD chart was calculated for the structure presented in Fig. 10a, next the structure was clockwise rotated 30° around the center and LFD chart was calculated once again. The results are presented in Fig. 10b. To facilitate the comparison, the second chart was rotated back by the same angle value. It's clearly visible, that the exact shape of the anisotropy chart depends on the orientation of the image even if the main anisotropy directions are preserved.

Contrarily to the MIL approach, in the case of LFD, the pixelization issue is negligible. Indeed, using this method, only the number of pixels belonging to each phase is counted through the sampling line, what is almost insensitive to false pixels ordering in the intercept point. Thus, only the disadvantage of square limited area needs to be corrected in the LFD method.

## 4 SOLUTIONS

### 4.1 Enhancements of the MIL method

Firstly, a simple solution eliminating both effects discussed in the previous section is proposed here. The idea is to ignore all pixels that are situated on the boundary. Because the area of near-phase boundary region is negligible comparing to the total area of the image, an appropriate mask can be created. The mask containing all pixels, having in the direct proximity pixels of two phases, is created. They are drawn in green in Fig. 11. In the improved method, the masked points are not considered during counting. Figure 11 illustrates the improvement obtained using this approach. The number of phase changes in the image treated without masking (Fig. 11a) is 14 and if the pixels on the border are omitted (masked), the number of phase changes decreased to 6 (Fig. 11b). It is quite a big difference, which significantly reduces the MIL value for a given angle.
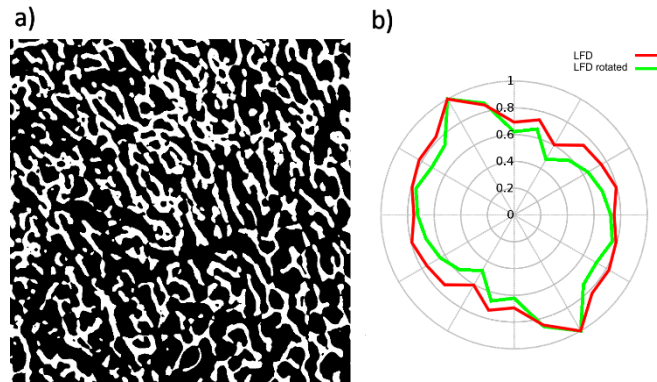
Figure 10: a) The testing image used in all test in this paper; b) anisotropy chart calculated for the testing image in original orientation and 30° rotated.

Secondly, using the improved MIL (i-MIL) method, the results for the tested images of Fig. 7a and Fig. 7b are significantly different. The plots for the 45°- rotated and not rotated ellipses are presented in Fig 12a. Now, both elliptic shapes (in red and green) are almost identical. Also, the comparison of i-MIL charts for low and high-resolution images illustrated in fig. 12b proves that the improvement guarantees identical i-MIL shapes independently from the resolution used.
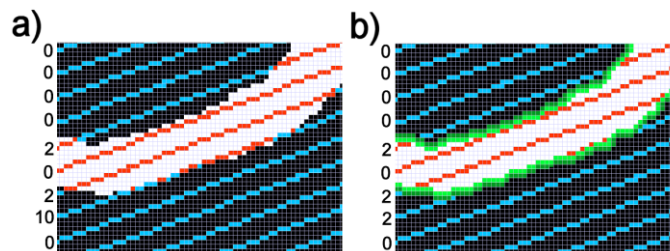


Figure 11: a) An image showing how the number of phase changes varies on "rough" and pixelized edges. b) Corrected image with masked pixels in green. The green colour pixels were eliminated from the counting process.

Finally, a good working method for anisotropy assessment should give similar shapes of anisotropy plots independently of the arbitrarily chosen orientation of the coordinate system. The orientation of the shape should follow the orientation of the coordinate system, but the shape itself should stay unchanged. The original and improved MIL are tested below for this feature. The testing image taken from computed tomography of the spongy bone (Fig. 13a) was rotated clockwise at 15˚ (Fig. 13b). For both images, the MIL and i-MIL plots were determined. To facilitate the comparison, the plots for the rotated images were rotated once again in the opposite direction. As it can be seen, the improved MIL method gives the same results independently from the rotation (Fig. 13d). It is not the case for the original MIL method (Fig. 13c) where the main direction of anisotropy is not kept and the shape of MIL function is different for images before and after rotation.

## 4.2 Improvement of the LFD method

In the improved LFD method (i-LFD), the whole area of the image is sampled independently of the scanning lines orientation.

The main source of the problem is that the calculation of the standard deviation of the phase fraction along the sampling line required that all lines have the same length. Therefore, for the classical method, the analyzed area is reduced to the small square inside the circle inscribed in the image. The idea to overcome the problem is to substitute the usual standard deviation

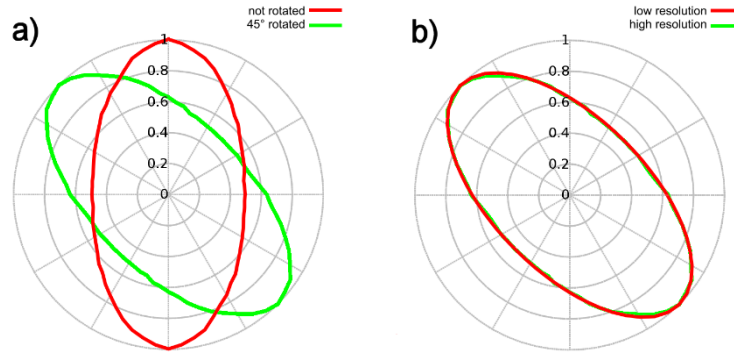calculation with a weighted standard deviation method.



Figure 12: a) i-MIL plots for rotated and not rotated ellipses. b) i-MIL plots for rotated low and high-resolution ellipses. Only one plot is visible because of the superimposition. Please compare with Fig. 6 for not improved MIL.

Let's make a statistical digression. There are two ways to calculate mean value $\bar{x}$ and the standard deviation $s$ depending on the data set we analyze. If we have the raw data (using a statistics term) for a single population, we use the following equations:

$$\bar{x} = \frac{\sum x_i}{n} \tag{3a}$$

$$s = \sqrt{\frac{1}{n} \cdot \sum (x_i - \bar{x})^2} \tag{3b}$$

In these equations, index i enumerates elements of population and n is the number of elements in population.

A different situation is met if our population is divided into several subpopulations with various numbers of elements in each one. In this case the equations below should be used:

$$\bar{x}_W = \frac{1}{\sum n_k} \cdot \sum n_k \cdot \overline{x_k} \tag{4a}$$

$$s_W = \sqrt{\frac{1}{N} \cdot \sum \frac{n_k}{\sum n_k} \cdot (\overline{x_k} - \bar{x}_W)^2} \tag{4b}$$

Symbols $\bar{x}_W$ and $s_W$ represent weighted mean value and weighted standard deviation respectively. Capital $N$ counts number of subpopulations, $n_k$ is a number of elements and $\bar{x}_k$ is a mean value in a subpopulation $k$. Please do not confuse the number of subpopulations N and the sum of all $n_k$ which corresponds to the number of all elements in each subpopulation.

The weighted standard deviation (eq. 4b) is used when it is needed to calculate the standard deviation of a set of data that are not equally significant. This method is applied, for example, to calculate the average salary in the European Community countries and standard deviation of this value. The average salary and its standard deviation in each of the countries should first be calculated using equations 3a and 3b. Next, the average salary in EC is determined according to equation 4a and the standard deviation according to equation 4b.

The same idea is applied to improve LFD method. The sampling lines are crossing the whole image independently of the direction (Fig. 14a). Of course, in this case, sampling lines have various lengths (like countries have various numbers of citizens). The new attempt to i-LFD determination is to calculate the standard deviation of the phase fraction for each angle of sampling lines but taking into account weighting factors, which are proportional to every single line length normalized by the sum of length of all lines. To verify the i-LFD method, a similar test as for i-MIL validation was performed. Namely, the method was applied to two identical

images but rotated 30⁰ one to another. After that, to facilitate the comparison, one of the anisotropy plots was rotated back. The resulting plots are shown in Fig. 14b. Two advantages are offered by the new proposition: for all angles of sampling lines, the entire sample is always analyzed and the rotation of the image has a much smaller influence on the i-LFD chart that it had in the case of classical LFD method the results of which are illustrated by Fig 10.
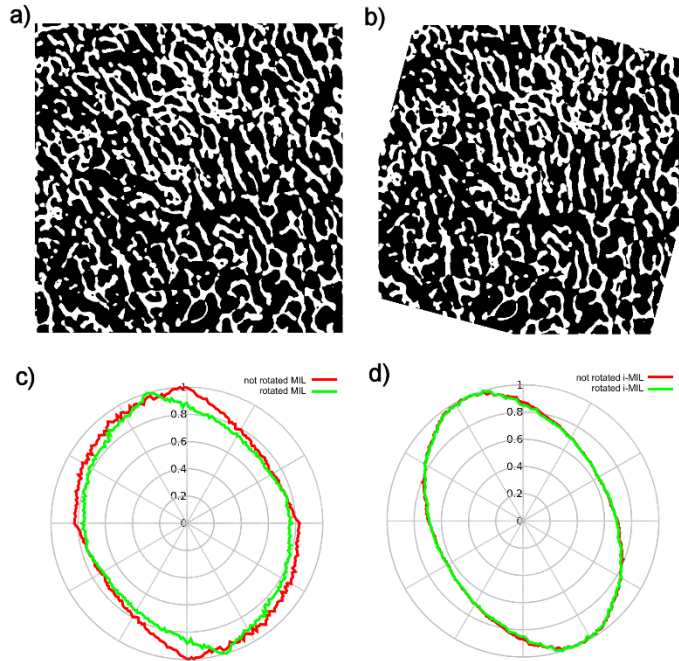


Figure 13: Influence of the image rotation on the results of the anisotropy assessment. The results for the rotated image (in both cases) were rotated back for an easier comparison: a) testing image, b) the same image rotated 15 degrees clockwise, c) original MIL plots, d) improved MIL plots.
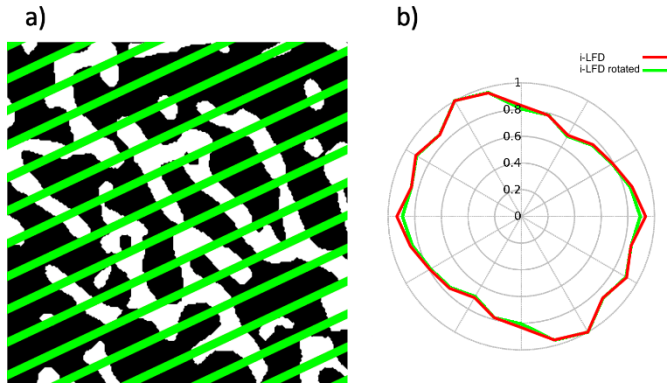


*Figure 14: a) Appearance of the test grid used in the improved LFD method for a selected angle. All areas of the image are always analyzed independently from the orientations of scanning lines.; b) i-LFD (improved LFD) method results.*

## 5  SUMMARY

Some important drawbacks of the classical methods for anisotropy determination, namely MIL and LFD, have been identified. Improvements have been proposed to overcome these insufficiencies. Firstly, a masking operation has been introduced in the i-MIL method to significantly eliminate the phase boundary roughness as well as the rasterization effects. There is a situation where the improved method should be used with care. For instance, in the case

where the image only contains small objects with the size of 1-3 pixels the whole structures may be masked. Such a configuration is however without any practical interest. Secondly, the weighted deviation calculated in i-LFD algorithm has shown to guarantee that the whole image area is analyzed for all scanning line directions.

Finally, for both improved methods proposed, anisotropy charts for the same original and rotated structures, are more similar than for classical algorithms.

## REFERENCES

[1] João Manuel R.S. Tavares, Renato M. Natal Jorge (eds.). *Lecture Notes in Computational Vision and Biomechanics*. Springer, 2018.

[2] F.O. Ribeiro, M.J. Gómez-Benito, J. Folgado, P.R. Fernandes, J.M. García-Aznar. Computational model of mesenchymal migration in 3D under chemotaxis. *Computer Methods in Biomechanics and Biomedical Engineering*, **20**(1), 59-74, 2017.

[1] Harris B. Engineering Composite Materials. London. The Institute of Metals, 1986

[2] Cowin S C. Bone poroelasticity. J Biomech. 32:218–238, 1999

[3] Wilmanski K. Permeability, tortuosity, and attenuation of waves in porous materials. Civil Environ Eng Res. 5:9–52, 2010

[4] Meyer GH. Die Architektur der Spongiosa. Arch Anat Phys wissensch Med, Reichert und DuBois-Reymonds Arch. 34:615–628, 1867

[5] Wolff J. Ueber die innere Architectur der Knochen und ihre Bedeutung fur die Frage vom Knochenwacbstum. Virchow Arch Pathol Anat Physiol Klin Med 50:389–450, 1870

[6] van Lenthe GH, Huiskes R. How morphology predicts mechanical properties of trabecular structures depends on intraspecimen trabecular thickness variations. J Biomech. 35:1191–1197, 2002

[7] Whitehouse W J. The quantitative morphology of anisotropic trabecular bone. J Micros. 101:153–168, 1974

[8] Geraets W G M. Computer aided analysis of the radiographic trabecular pattern. Thesis. Amsterdam: Vrije Universiteit, 1994

[9] Odgaard A, Jensen E B, Gundersen, H J G. Estimation of structural anisotropy based on volume orientation. A new concept. J Micros, 157: 149–162, 1990

[10] Cruz-Orive LM, Karlsson LM, Larsen SE, Wainschtein F. Characterizing anisotropy: a new concept. Micron Microsc Acta. 23:75–76, 1992

[11] Smit T H, Schneider E, Odgaard A. Star length distribution: a volume-based concept for the characterization of structural anisotropy. J Micros. 191:249–257, 1998

[12] Zysset P K, Ominsky M S, Goldstein S A. A Novel 3D Microstructural Model for Trabecular Bone: I. The Relationship between Fabric and Elasticity. Comput Methods Biomech Biomed Engin. 1:321–331, 1998

[13] Geraets W G M, Van der Stelt P F, Lips P, Elders P J M, Van F C. Orientation of the trabecular pattern of the distal radius around the menopause. J Biomech. 30:363–370, 1997

[14] Korstjens C M, Geraets W G M, Van Ginkel FC, Prahl-Andersen B, Van der Stelt P F, Burger E H. An analysis of the orientation of the radiographic trabecular pattern in the distal radius of children. Growth Dev Aging. 58:211–221, 1994